ISSN 1070–3632, Russian Journal of General Chemistry, 2014, Vol. 84, No. 6, pp. 1225–1236. © Pleiades Publishing, Ltd., 2014.

Application of Charge-Transfer Complexation for Evaluation of the Drug-Receptor Mechanism of Interaction: Spectroscopic and Structure Morphological Properties of Procaine and Pilocarpine Complexes with Chloranilic Acid Acceptor[1]

Abdel Majid A. Adam

Department of Chemistry, Faculty of Science, Taif University, Al-Haweiah, P.O. Box 888, Zip Code 21974, Taif, Saudi Arabia
e-mail: majidadam@yahoo.com

Received April 25, 2014

Abstract—Study of the charge-transfer or proton-transfer interaction of drugs is important for understanding the drug-receptor interactions and the mechanism of drug action. In the current research the corresponding data were accumulated in the course of synthesis and study of the H-bonded complexes originated from the interaction between procaine (Pro) or pilocarpine (Pil) drugs and chloranilic acid (CLA). The targeted microstructure products have been isolated and characterized by elemental and spectral (electronic and vibrational) data. Microstructural properties of the reported complexes were studied with XRD and SEM techniques. The Pil drug containing complex exhibited a specific electronic spectrum with a strong, broad absorption band with much longer wavelength, $\lambda_{max,}$ than those typical for the individual reagents. It is noteworthy that the complex had good crystallinity. Application of Debye–Scherrer equation indicated that the reported complexes were in the range of nanosize.

Keywords: drug-acceptor interaction; hydrogen bonds; XRD; SEM; surface structure

DOI: 10.1134/S1070363214060292

INTRODUCTION

Over the recent decade a big number of studies reported drug-acceptor interactions in solid state and in solutions. The study of the drug-acceptor complexation is useful for understanding the drug-receptor interactions and the mechanism of drug action. Furthermore, the drug-acceptor complexation is an important technique that is cheaper, simpler, and more efficient than the methods of drug determination described in a number of publications. The crystalline drug-acceptor complexes play a vital role in biological systems such as antimicrobial activity and DNA-binding. Beyond that, such complexes exhibit potential antimicrobial properties against Gram-positive and Gram-negative bacteria as well as fungi [1–11]. In the current study the drug-acceptor interaction between drug procaine or pilocarpine and chloranilic acid (CLA) acceptor is reported. Procaine hydrochloride (Pro; $C_{13}H_{20}N_2O_2 \cdot HCl$), chemically 2-(diethylamino) ethyl-4-aminobenzoate hydrochloride, the structure of which is shown in Scheme 1, is a synthetic local anesthetic drug of the amino ester family that produces a reversible loss of sensitivity by diminishing the conduction of sensory nerve impulses. It has long been employed as a pharmacological agent in the life science and in clinical therapeutic studies. This drug is primarily used to reduce pain induced by the intramuscular injection of penicillin, and it is also used in dentistry [12–14]. Pilocarpine hydrochloride (Pil; $C_{11}H_{16}N_2O_2 \cdot HCl$), chemically (3*S*,4*R*)-3-ethyl-4-[(1-methyl-1*H*-imidazol-5-yl)methyl]dihydrofuran-2(3*H*)-one, the structure of which is shown in Scheme 1, is a naturally occurring compound derived from the leaves of South American shrub *Pilocarpus jaborandi*. It is a parasympathomimetic agent that acts primarily as a muscarinic agonist with mild beta-adrenergic activity. This alkaloid causes pharmacologic stimulation of exocrine glands in humans, leading to diaphoresis, salivation, lacrimation, and gastric and pancreatic

[1] The text was submitted by the author in English.

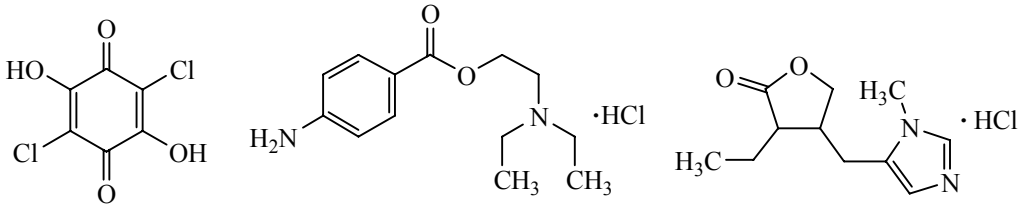

Chloranilic acid Procaine Pilocarpine

Scheme 1. The chemical structures of CLA, Pro, and Pil.

secretion. Topical ophthalmic pilocarpine has long been used to treat glaucoma [15, 16]. Based on the fruitful data of the complexation properties of drug-acceptor that had been accumulated by me [17–19], I carried out more studies of drug compounds. Accumulation of basic data that could be useful for understanding drug-receptor mechanism of interaction, the following objectives were pursued:

(1) Synthesis of the H-bonded complexes of Pro or Pil drugs with CLA acceptor.

(2) Study of the complexes formed based on elemental analysis and spectroscopic data (electronic and vibrational).

(3) Analysis of the microstructures of the reported complexes using XRD and SEM techniques.

EXPERIMENTAL

General. All compounds used throughout this study were of analytical reagent grade and all solutions were freshly prepared. Pro, Pil, CLA, and methanol (Aldrich and Merck Chemical) were used without further purification. The elemental analyses of carbon, hydrogen and nitrogen content were performed with a Perkin-Elmer CHN 2400 (USA). The electronic absorption spectra of the reagents and complexes synthesized were recorded in methanol over a wavelength range of 250–800 nm using a Perkin-Elmer Lambda 25 UV/Vis double-beam spectrophotometer. The instrument was fitted with a quartz cell that had a path length of 1.0 cm. The IR spectra of the corresponding KBr tablets were recorded within the range of 4000–400 cm^{-1} at room temperature using a Shimadzu FT-IR spectrophotometer with 30 scans at 2 cm^{-1} resolution. The diffraction experiments were carried out with a PANalytical X'Pert PRO X-ray powder diffractometer with a Ge(III) monochromator. A Cu$K_{\alpha 1}$ X-ray beam of wavelength 0.154056 nm was used. The samples were measured in 0.35 mm diameter glass capillaries at room temperature. Scanning electron micrography (Quanta FEG 250) instrument was used for morphological evaluation. The instrument was operated at an accelerating voltage of 30 kV.

Synthetic procedure. The solid H-bonded complexes were prepared by mixing the saturated solution of the drug (1 mmol) in pure methanol (25 mL) with saturated solution of CLA acceptor (1 mmol) also in methanol (25 mL). The solutions were stirred for approximately 30 min. A change in color developed and the resulting solution was allowed to evaporate slowly at room temperature to lead to precipitation of the solid complexes. The formed precipitate was filtered off and rinsed well with methanol. Then, the complexes were dried in vacuum over anhydrous calcium chloride for 24 h. The melting point of the formed complexes was measured to be >300°C. The H-bonded complexes were characterized spectrophotometrically (IR and UV-vis) and by elemental analysis.

Spectrophotometric measurements. The spectrophotometrically controlled titrations of the detectable absorption bands were performed for the reactions of the drugs with CLA acceptor as follows. Portions of 0.25, 0.50, 0.75, 1.00, 1.50, 2.0, 2.50, 3.00, 3.50 or 4.00 mL of a standard solution (5.0×10^{-4} M) of the CLA acceptor in methanol was added to 1.00 mL of 5.0×10^{-4} M Pro or Pil, dissolved in the same solvent. The final volume of the mixture was 5 mL. The concentration of the drug (C_d) was maintained at 5.0×10^{-4} M, whereas the concentration of the acceptor (C_a) varied from 0.25×10^{-4} M to 4.00×10^{-4} M to produce solutions with a (drug : acceptor) molar ratio range between 1 : 0.25 and 1 : 4. The stoichiometry of the formed complexes was evaluated by determination of the conventional spectrophotometric molar ratio according to a known method [20]. The peak absorbencies that appeared in the spectra of the formed complexes were measured for all solutions in each case

Table 1. Spectroscopic data for the H-bonded complexes in methanol at room temperature

Complex	Color	Absorption, nm	K, L mol^{-1}	e_{max}, L mol^{-1} cm^{-1}	E_{CT}, eV	f	μ	ΔG^0, J mol^{-1}
[(Pro)(CLA)]	Dark red	334	1.59×10^4	8.45×10^3	4.20	32.87	44.69	–35.731
[(Pil)(CLA)]	Dark orange	320	1.44×10^4	3.32×10^4	4.33	21.60	38.05	–32.458

and plotted as a function of the drug to acceptor molar ratio (C_d : C_a ratio).

RESULTS AND DISCUSSION

Analytical results. The result of the elemental analyses (C, H, and N) of the formed H-bonded complexes is presented as; [(Pro)(CLA)]: $C_{19}H_{23}N_2O_6Cl_3$; M_w = 481.76; Calculated, %: C 47.33; H 4.77; N 5.81, Found, %: C 47.20; H 4.81; N 5.77. [(Pil)(CLA)]: $C_{17}H_{19}N_2O_6Cl_3$; M_w = 453.7; Calculated, %: C 44.96; H 4.19; N 6.17. Found, %: C 44.90; H 4.15; N 6.21. Elemental analysis justified formation of the Pro and Pil complexes of the type [(Drug)(CLA)]. Formation of 1 : 1 complexes was strongly supported by spectrophotometric titrations. The Pro and Pil complexes had a dark red and dark orange color, respectively.

Electronic spectra. The Spectroscopic data, molar ratio and color of the formed H-bonded complexes are presented in Table 1. The electronic absorption spectra of the reactants, drugs (Pro and Pil) (5.0×10^{-4} M) and CLA acceptor (5.0×10^{-4}), along with those of the synthesized complexes are presented in Fig. 1. The spectrum of the Pro complex revealed the presence of a new broad band at 334 nm that was assigned to the drug-acceptor interaction. Spectrophotometric titration curve based on this absorption band justified a reaction stoichiometry of 1 : 1 (Pro : CLA) as shown in Fig. 2. The absorption spectrum of CLA acceptor had a λ_{max} at 303 nm, while Pil drug displayed no detectable absorption band. Upon mixing Pil and CLA together, a new strong broad band appeared at a much longer wavelength (320 nm). This strong broad band at longer wavelength was indicative of the formation of the H-bonded complex. The composition of the formed complex was determined by spectrophotometric titrations based on this characteristic absorption band. Accordingly, it is evident from Fig. 2 that this complex had a 1 : 1 stoichiometric ratio (Pil : CLA). This was in good agreement with the elemental analysis data of the resulting solid complex.

Calculation of *K* and ε. Based on the electronic spectra of the synthesized H-bonded complexes, the formation constant; K (L mol^{-1}) and the molar

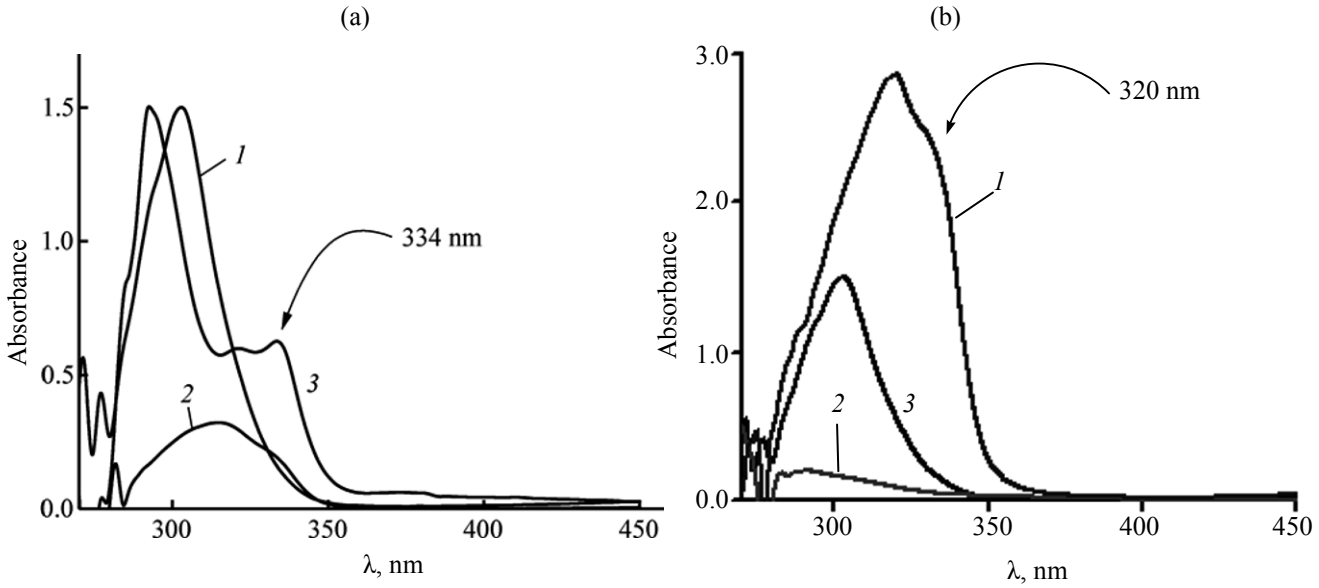

Fig. 1. Electronic spectra of (a) Pro and (b) Pil complexes in methanol solution. (*1*) CLA, (*2*) Pil, and (*3*) complex.

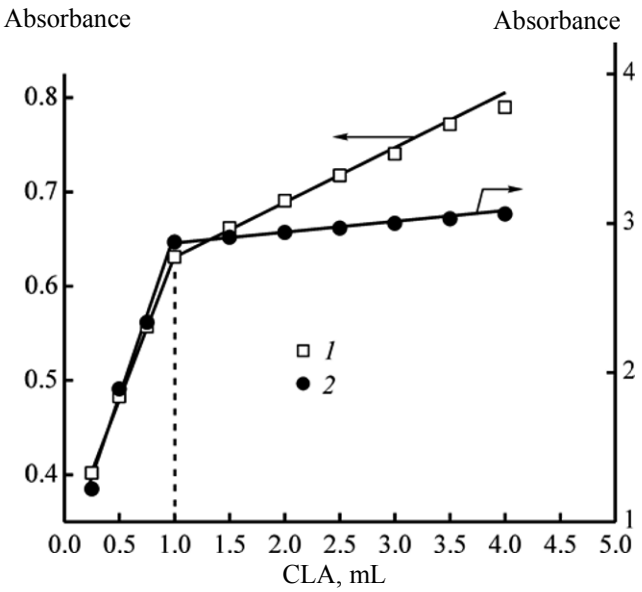

Fig. 2. Spectrophotometric titration curves of (*1*) Pro and (*2*) Pil complexes in methanol solutions.

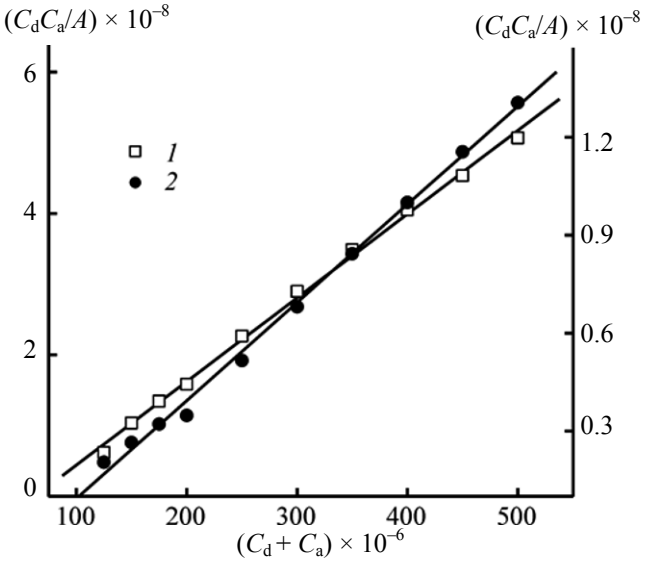

Fig. 3. The Benesi–Hildebrand plot of (*1*) Pro and (*2*) Pil complexes.

extinction coefficient; ε (L mol^{-1} cm^{-1}) were calculated using the 1 : 1 Benesi–Hildebrand equation:

$$(C_aC_d)/A = 1/K\varepsilon + (C_a + C_d)/\varepsilon, \quad (1)$$

where C_a and C_d are the initial concentrations of the acceptor (CLA) and the drug, respectively, while A is the absorbance at the mentioned absorption band. By plotting the values of $(C_aC_d)/A$ as a function of the corresponding values of $(C_a + C_d)$, a straight line was produced, which supports the formation of a 1 : 1 complex. In the plot, the slope and intercept were measured as $1/\varepsilon$ and $1/K\varepsilon$, respectively. The Benesi–Hildebrand plots are shown in Fig. 3, and the values of C_d, C_a, $(C_d + C_a)$ and $(C_aC_d)/A$ are listed in Table 2. The correlation coefficient (r) value for the straight line was found to be 0.999. The values of the K for the Pro and Pil complexes were calculated to be 1.59×10^4, and 1.44×10^4 L mol^{-1}, respectively. The corresponding

Table 2. The values of C_d, C_a, $C_d + C_a$, and C_dC_a/A, for the formed complexes

A : D ratio	$C_d \times 10^{-4}$	$C_a \times 10^{-4}$	$(C_d + C_a) \times 10^{-6}$	$(C_dC_a) \times 10^{-8}$	Pro–CLA complex		Pil–CLA complex	
					absorbance (334 nm)	$[(C_dC_a)/A] \times 10^{-8}$	absorbance (320 nm)	$[(C_dC_a)/A] \times 10^{-8}$
0.25	1.00	0.25	125	0.25	0.4018	0.6222	1.2212	0.2047
0.50	1.00	0.50	150	0.50	0.4829	1.0354	1.8900	0.2646
0.75	1.00	0.75	175	0.75	0.5569	1.3467	2.3357	0.3211
1.00	1.00	1.00	200	1.00	0.6309	1.5850	2.8745	0.3479
1.50	1.00	1.50	250	1.50	0.6618	2.2665	2.9066	0.5161
2.00	1.00	2.00	300	2.00	0.6905	2.8965	2.9391	0.6805
2.50	1.00	2.50	350	2.50	0.7172	3.4858	2.9664	0.8428
3.00	1.00	3.00	400	3.00	0.7405	4.0513	2.9988	1.0004
3.50	1.00	3.50	450	3.50	0.7717	4.5354	3.0293	1.1554
4.00	1.00	4.00	500	4.00	0.7896	5.0659	3.0630	1.3059

Table 3. IR spectral data (cm^{-1}) and tentative assignments of donors, acceptor and complexes

Acceptor	Donors		Complexes		Assignments
CLA	Pro	Pil	Pro–CLA	Pil–CLA	
–	3349	–	3386	–	ν(N–H); Pro
3230	–	–	3163	3077	ν(OH); CLA
–	3206	–	2961	–	ν(C–H); aromatic
–	2973	3108 3021	2865	3023 2990	ν_s(C–H) + ν_{as}(C–H)
–	–	–	2728 2683	2708 2667 2600 2554	Hydrogen bonding
–	2583 2493	–	2615	–	ν($^+$N–H); hydrogen of HCl
1663 1629	1692	1761 1671	1714	1760	ν(C=O); Pro, Pil
–	1644	–	1631	–	δ_{def}(N–H); Pro
–	1603	1615	1528	1609	ν(C–N); Pro, Pil
–	–	1584	–	1561	ν(C=N); Pil
–	1520 1463	1442	1438 1376	1450	ν(C–H); alkanes; Pro, Pil
1368 1260	1363 1308 1268	1362 1315 1240	1338 1270	1393 1329 1281 1225	ν(C–C) + ν(C–O) + ν(C–N)
–	1169 1113	1172 1114	1181 1117	1175	C–H in-plane bending
–	1049	–	1011	–	δ_{rock}, NH; Pro
–	848	1021 982	977 836	1025 928	C–H out of plane bending
838	–	–	805	820	ν(C–Cl); CLA
751	–	–	717	715	ν(C–Cl); CLA

ε values were 8.45×10^3 and 3.32×10^4 L mol^{-1} cm^{-1}, respectively. These results indicated that Pro complex exhibited a higher *K* value then that of Pil complex, which indicates a strong interaction between the Pro–CLA pairs and confirmed high stability of the Pro complex as a result of the stroger donation ability of Pro drug. Accordingly, donation from the drug to CLA acceptor was in the order Pro > Pil. The Pil complex exhibited a higher ε value than Pro complex.

Calculation of the spectroscopic data. The spectroscopic data, such as the energy of the complex (*E*), the oscillator strength (*f*), the transition dipole moment (μ) and the standard free energy (ΔG^0), were estimated for the formed complexes dissolved in methanol at 25°C. The calculations are summarized below.

The energy values of the complexes (*E*) of the $n \rightarrow \pi^*$ and π–π^* interactions between the drug donors and the acceptor were calculated using the equation derived by Briegleb [21]:

$$E_{CT} = (h\nu_{CT}) = 1243.667/\lambda_{CT}, \quad (2)$$

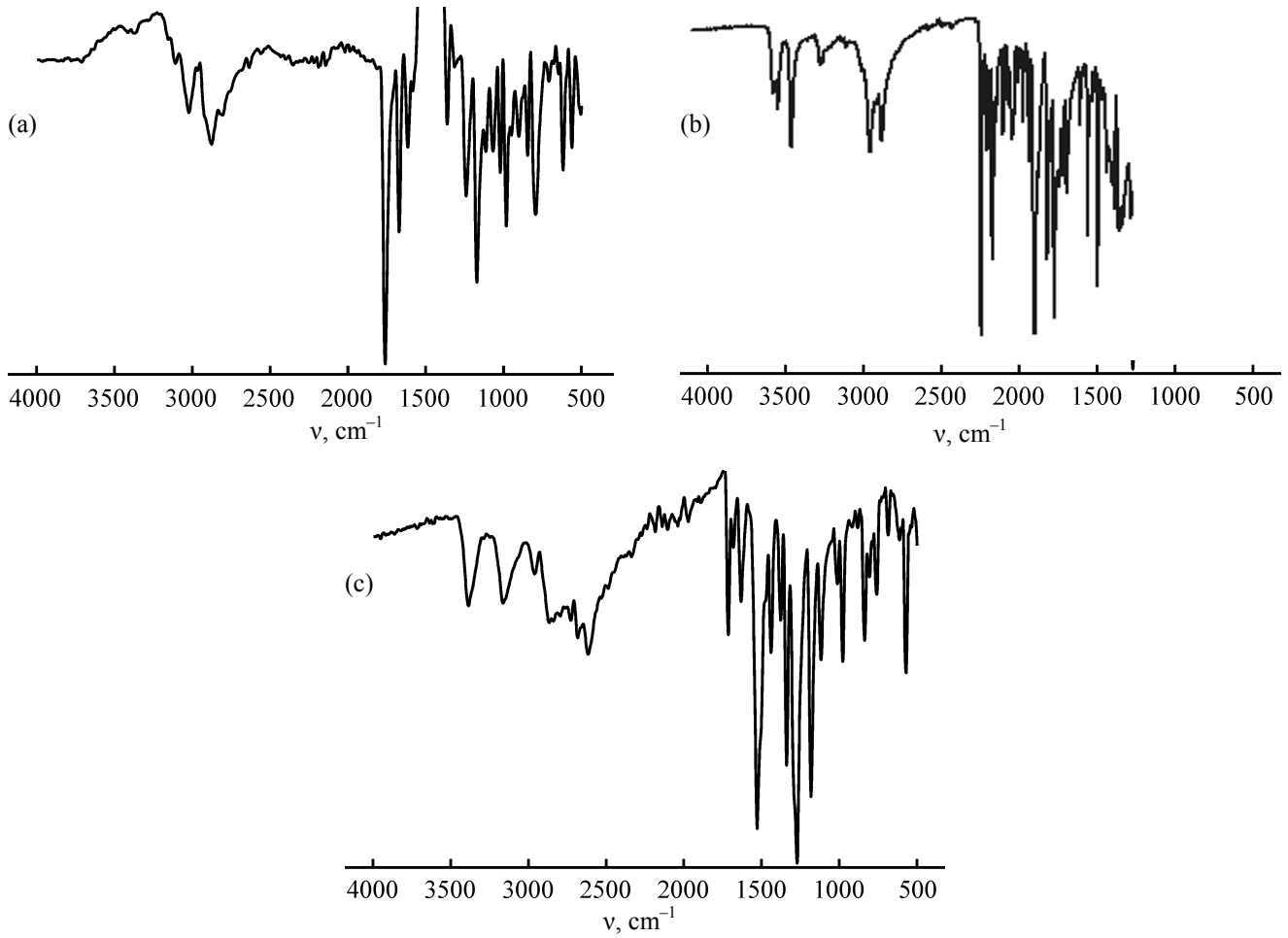

Fig. 4. Infrared spectra of (a) CLA, (b) Pro, and (c) the their complex.

where λ_{CT}, nm, is the wavelength of the complexation band.

The oscillator strength (*f*) is a dimensionless quantity used to express the transition probability of the band. From the absorption spectra, the oscillator strength (*f*) can be calculated using the approximate formula [22]:

$$f = 4.319 \times 10^{-9} \int \varepsilon_{CT} d\nu, \quad (3)$$

where $\int \varepsilon_{CT} d\nu$ is the area under the curve of the extinction coefficient of the absorption band plotted as a function of the frequency. To a first approximation,

$$f = 4.319 \times 10^{-9} \varepsilon_{CT} \nu_{1/2}, \quad (4)$$

where ε_{CT} is the maximum extinction coefficient of the CT band and $\nu_{1/2}$ is the half-bandwidth (i.e., the bandwidth at half of the maximum extinction coefficient value), cm^{-1}.

The transition dipole moments (μ) of the complexes were calculated in accodance with Eq. (5) [23]:

$$\mu(\text{Debye}) = 0.0958 [\varepsilon_{CT} \nu_{1/2} / \nu_{max}]^{1/2}. \quad (5)$$

The transition dipole moment (μ) can be determined if a particular transition is allowed. The transition from a bonding π orbital to an antibonding π^* orbital is allowed because the integral that defines the transition dipole moment is nonzero.

The standard free energy changes of complexation (ΔG^0) for each complex were calculated based on the formation constants using Eq. (6) [24]:

$$\Delta G^0 = -2.303 RT \log K_{CT}, \quad (6)$$

where ΔG^0 is the standard free energy change of the complexes (kJ/mol), *R* is the gas constant (8.314 J $mol^{-1} K^{-1}$), *T* is the absolute temperature in Kelvin, and *K* is the formation constant of the complex (L mol^{-1}) at room temperature.

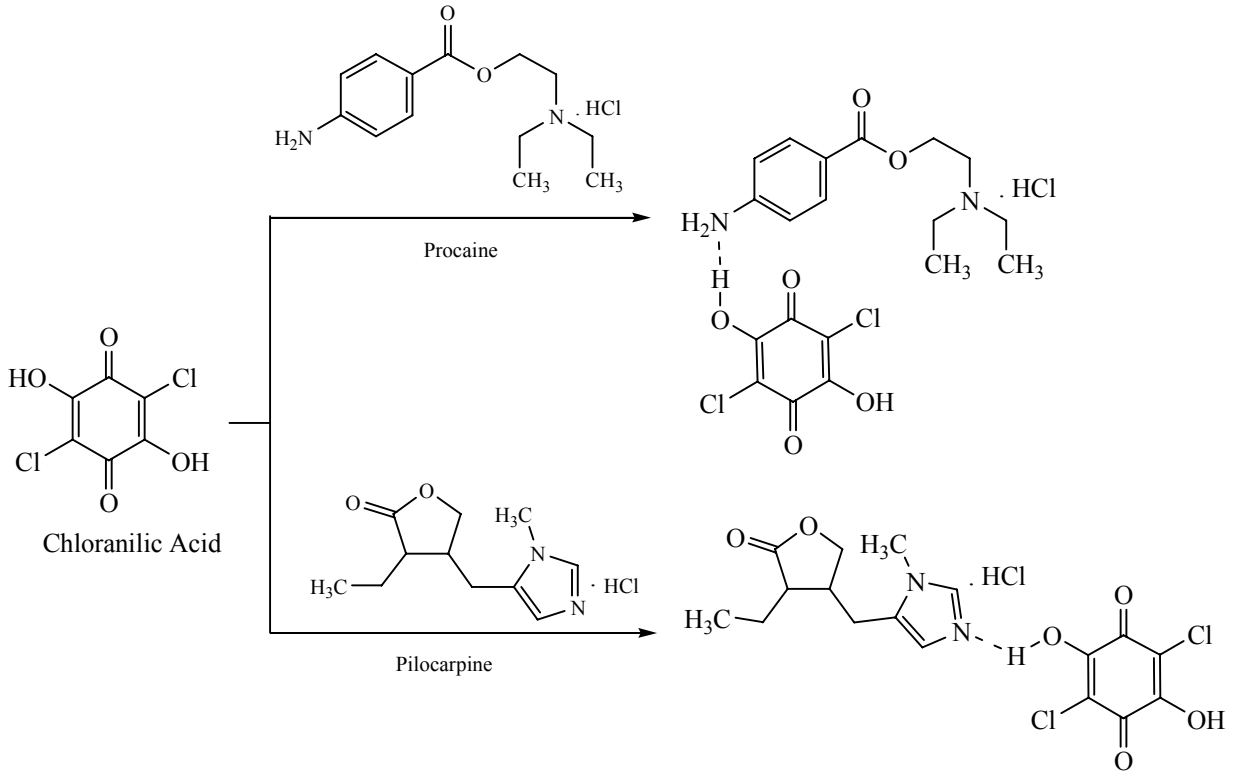

Scheme 2. Proposed structure of the reported complexes.

The calculated values of the spectroscopic data for the reported complexes deduced from Eqs. (2)–(6) are presented in Table 1. The Pro complex exhibited a higher value for both the oscillator strength (*f*) and the transition dipole moment (μ). All the ΔG^0 values are negative. These values indicate that the interaction between the drug donors and the CLA acceptor was spontaneous. The ΔG^0 values of the complexes are in the order Pro > Pil.

IR spectral studies. The infrared spectra of the Pro and CLA as well as the formed complex are presented in Fig. 4, and the corresponding bands are listed in Table 3. However, the appearance of a group of IR bands in the spectrum of Pro complex supported the conclusion that a deformation of the electronic environment of the complex occurred due to formation of intermolecular H-bond. The characteristic band of ν(N–H) at 3349 cm^{-1} in the free Pro drug was shifted to 3386 cm^{-1} in the complex. The outlined changes in ν(N–H) in the Pro drug upon complexation clearly justified the involvement of the nitrogen atom of the ($–NH_2$) group in hydrogen bonding with CLA. This bonding was confirmed by the appearance of weak absorption bands at 2728 and 2683 cm^{-1}, assigned to the H-bonded OH group. Also, the δ_{def}(N–H) vibration at 1644 cm^{-1} characteristic for free Pro drug, was shifted to 1631 cm^{-1} in the spectrum of the product confirming the complex formation. In the spectrum of the complex ν(C–Cl) bands were recorded at 805 and 717 cm^{-1} whereas in pure CLA the corresponding bands were recorded at 838 and 751 cm^{-1}. All these observations indicated the formation of intermolecular H-bond between the ($–NH_2$) group in the Pro drug and the (–OH) group in the CLA acceptor [25–28].

Figure 4 presents the IR spectra of the Pil, CLA and their solid complex, and Table 3 their characteristic band assignments. As expected, the characteristic IR bands of Pil and CLA in the complex exhibited small changes in the band intensities and frequency values. The IR spectrum of this complex was characterized by a group of bands that appears in the range 2554–2708 cm^{-1}. This group of bands was not registered in the spectra of pure Pil or CLA, and was attributed to the stretching vibration of protons attached to the donation center of the Pil (electrons lone pair on the nitrogen atom of the C=N group). This was supported by a shift of ν(C=N) band from 1584 cm^{-1} (in pure Pil) to 1561 cm^{-1} (in the complex). Furthermore, ν(C–Cl)

Table 4. XRD spectral data for the reported complexes

Complex	Position 2θ, deg	*d*-Spacing value, Å	Relative intensity, %	β; FWHM	Particle size, nm
[(Pro)(CLA)]	8.41640	10.50592	100.0	0.3499	47.578
[(Pil)(CLA)]	17.9388	4.940770	100.0	0.2362	71.163

vibrational bands were recorded at 820 and 715 cm^{-1} in the spectrum of the complex. In pure CLA those were recorded at 838 and 751 cm^{-1}. These data stood for the intermolecular H-bond formation in the complex [25–28]. Based on the above, the H-bonds between the drugs and the CLA acceptor are presented in Scheme 2.

XRD characterization. The X-ray diffraction (XRD) patterns were recorded for 2θ = 5°–80° at a scanning speed of 3 deg/min using a PANalytical model X'PERT-PRO X-ray powder diffractometer system. The XRD patterns of the reported complexes are shown in Fig. 5. The mean particle size of the complexes based on the highest intensity line (Fig. 6) were calculated using the Debye–Scherrer formula [29]:

$$D = 0.94\lambda / \beta \cos \theta, \quad (7)$$

where D is the mean particle size of the grains, 0.94 in the Scherrer constant; λ is the wavelength of the incident X-ray (CuK_α; 1.5406 Å), θ is the position of the selected diffraction peak (Bragg diffraction angle) and β is the full-width at half-maximum (FWHM) of the selected diffraction peak in radians. Table 4 presents the XRD spectral data [i.e., 2θ, β, d (the interplanar spacing between atoms) and D in nm] for the obtained complexes, whereas Table 5 lists all the characteristic XRD lines with their d-spacing, FWHM and relative intensity.

The XRD study produced the following results:

(1) The primary characteristic scattering peak of the Pro and Pil complexes occurred at 8.4164° and 17.9388° in the diffraction pattern, respectively.

(2) The XRD patterns of the Pro and Pil complexes differed from each other.

(3) The appearance of a sharp and strong Bragg peak indicated the formation of a well-defined crystalline structure.

(4) Using the Debye–Scherrer equation, the particle size values of the complexes were calculated to be 47.6 and 71 nm for the [(Pro)(CLA)] and [(Pil)(CLA)] complexes, respectively.

(5) The above values indicated nanoscale particle sizes.

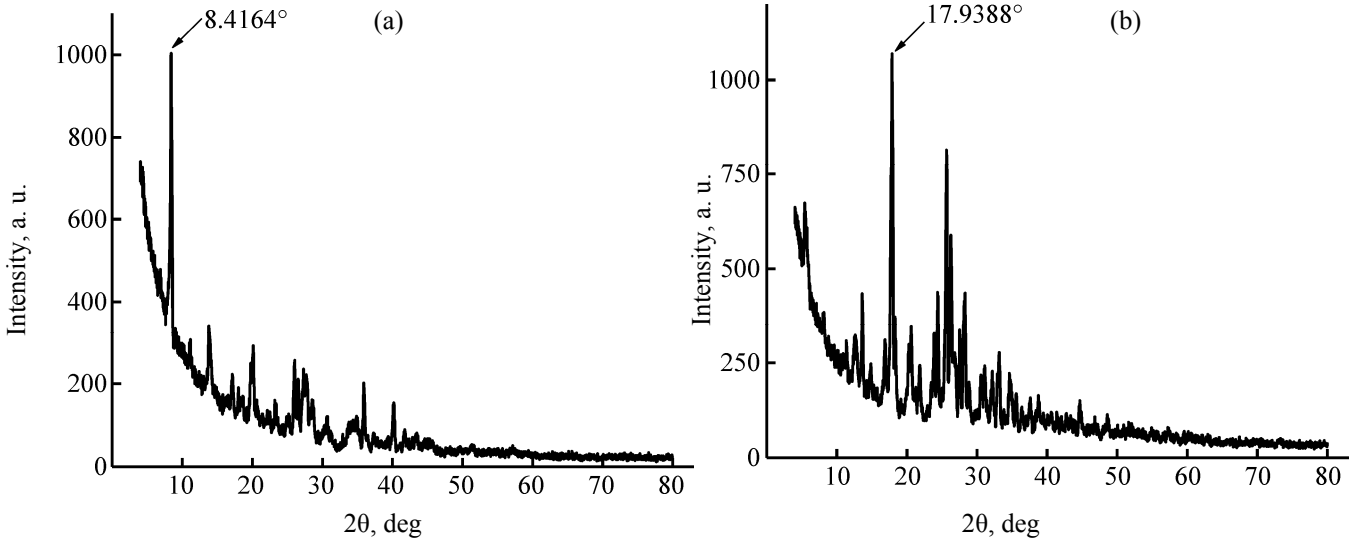

Fig. 5. X-ray diffraction patterns of (a) Pro and (b) Pil complexes.

Table 5. Characteristic XRD lines for the reported complexes

[(Pro)(CLA)] complex				[(Pil)(CLA)] complex			
position 2θ, deg	*d*-spacing value, Å	relative intensity, %	FWHM	position 2θ, deg	*d*-spacing value, Å	relative intensity, %	FWHM
8.4164	10.50592	100.00	0.3499	5.4764	16.12439	21.87	0.3936
11.1186	7.95796	29.56	0.6071	8.1033	10.90210	4.70	0.4723
13.8221	6.40696	33.15	0.3335	11.3888	7.76333	6.56	0.2362
17.1639	5.16632	21.47	0.4378	12.5657	7.03878	13.63	0.3542
20.0994	4.41792	27.53	0.3952	13.6407	6.48635	27.21	0.2165
23.3061	3.81681	14.55	0.5414	14.8139	5.97519	7.74	0.3149
26.0292	3.42336	24.94	0.3154	16.8869	5.24609	19.58	0.2165
27.7349	3.21657	21.43	0.8964	17.9388	4.94077	100.00	0.2362
28.4300	3.13949	13.20	0.0010	18.2903	4.84660	25.47	0.1574
30.6500	2.91697	11.08	0.0010	20.6046	4.30716	25.42	0.1968
35.9300	2.49950	18.60	0.2164	21.8336	4.06741	13.61	0.2362
40.1733	2.24475	14.68	0.2050	23.8732	3.72432	24.93	0.2165
41.7900	2.16157	4.92	0.0900	24.4008	3.64498	39.91	0.2362
				25.6435	3.47109	87.84	0.2362
				26.2891	3.38729	60.69	0.2558
				26.9040	3.31125	17.98	0.2558
				27.5739	3.23231	23.89	0.1771
				28.2527	3.15618	39.20	0.1968
				28.9062	3.08629	9.01	0.2362
				30.5651	2.92246	11.73	0.2362
				31.0597	2.87704	16.07	0.2165
				32.1874	2.77877	12.51	0.3936
				33.1810	2.69779	20.69	0.2362
				34.5746	2.59218	12.47	0.3149
				35.5808	2.52114	8.46	0.2558
				36.3304	2.47083	3.77	0.3149
				37.5787	2.39157	7.28	0.3140
				38.6639	2.32690	5.85	0.6298
				44.5958	2.03019	7.87	0.2755
				48.6633	1.86958	4.54	0.3840

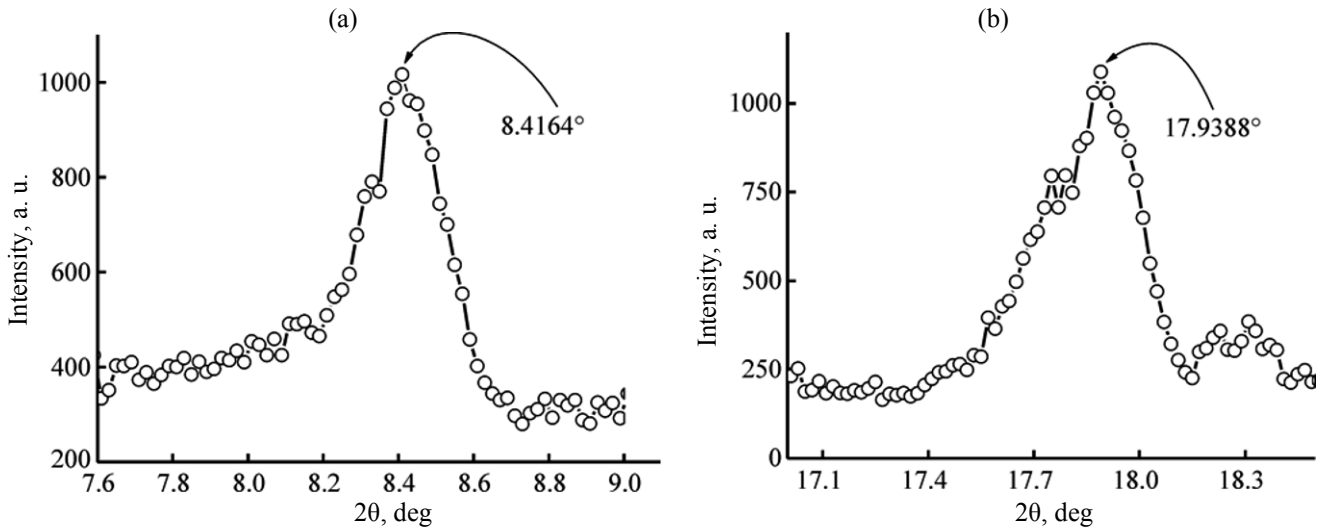

Fig. 6. The highest intensity XRD line of the (a) Pro and (b) Pil complexes.

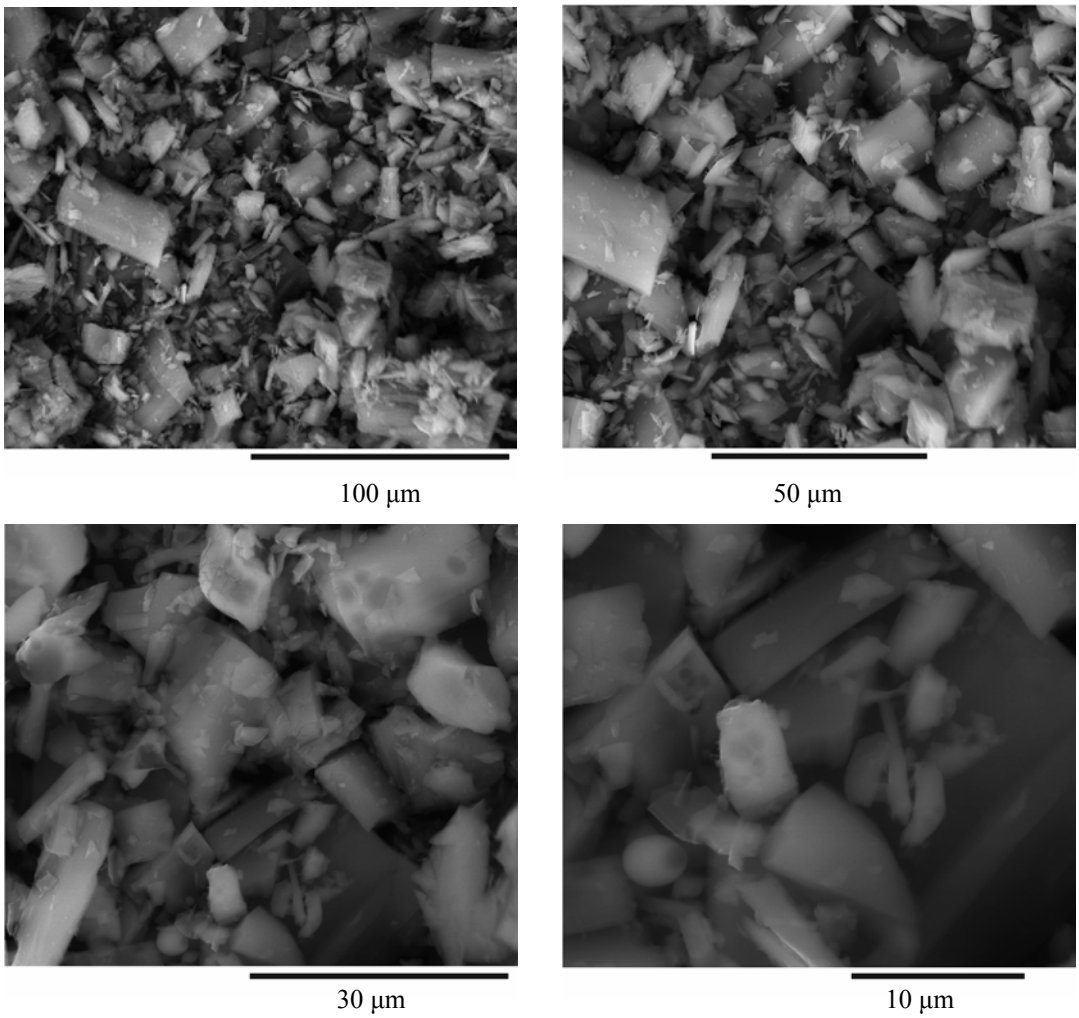

Fig. 7. SEM photographs of Pro complex at various magnifications.

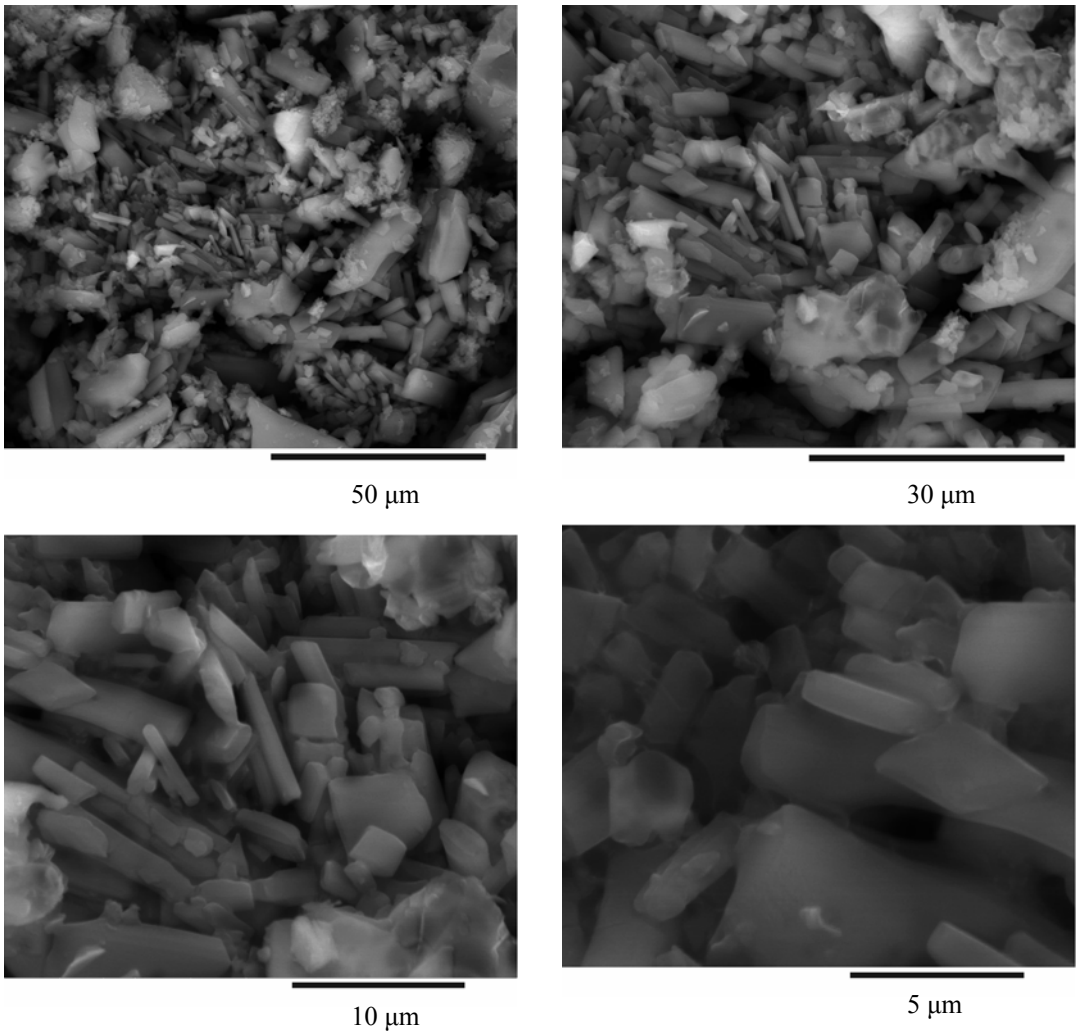

Fig. 8. SEM images of Pil complex at various magnifications.

Surface morphology characterization. Morphology of the new H-bond supported complexes was studied by means of scanning electron microscopy (SEM) technique. The surface images obtained with the SEM technique provided general information regarding the microstructure, surface morphology, particle size, chemical composition, and porous structures of the surfaces. The morphological phases of the formed H-bonded complexes revealed some uniform matrixes in the SEM micrographs indicating the formation of a homogeneous material. Morphological difference was observed between Pro and Pil complexes. Pil complex exhibited a higher degree of crystallinity than that of Pro complex. The size of the particles differed substantially for each drug. Figure 7 presents the SEM photographs of the Pro complex at various magnifications. The photographs demonstrated the presence of agglomerated particles with irregular shape and sizes with the latter in the range of 10–50 μm. Some higher magnification SEM photographs of representative complex are displayed. The highly magnified SEM image demonstrated the presence of particles with shape close to spherical. Some particles of imperfect structures could also be observed in the matrix. Figure 8 displays the surface morphology of the nanoscale Pil complex. The complexation of Pil with CLA led to a very interesting morphology. The multi SEM photographs with various degrees of magnification of the complex indicated rod-like structure with particles size in the range of 5–10 μm. A SEM photograph at a high magnification (×20 000) demonstrated a well-defined microstructure. This image demonstrated complex homogeneous surface with clear individual grins of uniformly

distributed size and shape. The morphology of Pro complex and Pil complex were of different microstructures.

CONCLUSIONS

Lately considerable attention has been paid to formation of stable charge-transfer (CT) complexes that resulted from the reaction of acceptors with drugs. This interest was initiated by important physical and chemical properties of such complexes. The CT complexes of procaine (Pro) and pilocarpine (Pil) drugs with chloranilic acid (CLA) were synthesized and studied spectroscopically in both solid and liquid phases at room temperature. The newly synthesized complexes were characterized in terms of elemental analysis, IR and UV-visible spectroscopy. Their microstructure characteristics were evaluated by means of XRD and SEM techniques. The reaction stoichiometry was 1 : 1, and the resulting CT complexes had the general formula: [(Drug)(CLA)]. Physical parameters such as formation constant (K_{CT}), molar extinction coefficient (ε_{CT}) and other spectroscopic data were calculated using the Benesi–Hildebrand method. The sharp, well-defined Bragg reflections at specific 2θ angles were identified from the powder X-ray diffraction patterns.

REFERENCES

1. Saravanabhavan, M., Sathya, K., Puranik, V.G., and Sekar, M., *Spectrochim. Acta A* 2014, no. 118, pp. 399–406.
2. Khan, I.M., Ahmad, A., and Ullah, M.F., *J. Photochem. Photobio. B,* 2011, no. 103, pp. 42–49.
3. Khan, I.M., Ahmad, A., and Ullah, M.F., *Spectrochim. Acta A,* 2013, no. 102, pp. 82–87.
4. Khan, I.M., Ahmad, A., and Aatif, M., *J. Photochem. Photobio. B,* 2011, no. 105, pp. 6–13.
5. Khan, I.M. and Ahmad, A., *J. Mol. Struct.,* 2010, no. 975, pp. 381–388.
6. Khan, I.M. and Ahmad, A., *J. Mol. Struct.,* 2010, no. 977, pp. 189–196.
7. Khan, I.M., Ahmad, A., and Kumar, S., *J. Mol. Struct.,* 2013, no. 1035, pp. 38–45.
8. Eldaroti, H.H., Gadir, S.A., Refat, S.A., and Adam, A.M.A., *Spectrochim. Acta A,* 2013, no. 115, pp. 309–323.
9. Eldaroti, H.H., Gadir, S.A., Refat, S.A., and Adam, A.M.A., *Spectrochim. Acta A,* 2013, no. 109, pp. 259–271.
10. Eldaroti, H.H., Gadir, S.A., Refat, S.A., and Adam, A.M.A., *J. Pharm. Anal.,* 2013, in press.
11. Eldaroti, H.H., Gadir, S.A., Refat, S.A., and Adam, A.M.A., *Int. J. Electrochem. Sci.,* 2013, no. 8, pp. 5774–5800.
12. Yuan, J., Yin, J., Wang, E., *J. Chromatogr. A,* 2007, no. 1154, pp. 368–372.
13. Chen, Y., Lu, K., Hsiao, R., Lee, Y., Tsai, H., Lin, C.H., and Tsai, M., *J. Comp. Biochem. Physiol. C,* 2008, no. 148, pp. 128–135.
14. Karadaş, Ö, Omaç, Ö.K., Tok, F., Özgül, A., and Odabaşı, Z., *J. Neurological Sci.,* 2012, no. 316, pp. 76–78.
15. Johnson, J.T., Ferretti, G.A., Nethery, W.J., Valdez, I.H., Fox, P.C., Ng, D., Muscoplat, C.C., and Gallagher, S.C., *N. Engl. J. of Med.,* 1993, no. 5, pp. 390–395.
16. Vivino, F.B., Al-Hashimi, I., Khan, Z., LeVeque, F.G., Salisbury, P.L., Tran-Johnson, T.K., Muscoplat, C.C., Trivedi, M., Goldlust, B., and Gallagher, S.C., *Arch. Intern. Med.,* 1999, no. 159, pp. 174–181.
17. Adam, A.M.A., *J. Mol. Struct.,* 2012, no. 1030, pp. 26–39.
18. Adam, A.M.A., Refat, M.S., Saad, H.A., and Eldaroti, H.H., *Eur. Chem. Bull.,* 2012, vol. 1(7), pp. 241–249.
19. Adam, A.M.A., Salman, M., Sharshar, T., and Refat, M.S., *Int. J. Electrochem. Sci.,* 2013, no. 8, pp. 1274–1294.
20. Skoog, D.A., *Principle of Instrumental Analysis*, 3 ed., Saunders College Publishing, New York, USA, 1985.
21. Briegleb, G., *Z. Angew. Chem.,* 1964, no. 3, pp. 617–632.
22. Tsubomura, H. and Lang, R.P., *J. Am. Chem. Soc.,* 1961, no. 83, pp. 2085–2092.
23. Rathone, R., Lindeman, S.V., and Kochi, J.K., *J. Am. Chem. Soc.,* 1997, no. 119, pp. 9393–9404.
24. Martin, A.N., Swarbrick, J., and Cammarata, V, *Physical Pharmacy*, 3 ed., Lee and Febiger, Philadelphia, PA, 1969, p. 344.
25. Adam, A.M.A., Refat, M.S., and Saad, H.A., *J. Mol. Struct.,* 2013, no. 1051, pp. 144–163.
26. Adam, A.M.A., Refat, M.S., and Saad, H.A., *J. Mol. Struct.,* 2013, no. 1037, pp. 376–392.
27. Adam, A.M.A., *Spectrochim. Acta A,* 2013, no. 104, pp. 1–13.
28. Khan, I.M. and Ahmad, A., *J. Mol. Struct.,* 2013, no. 1050, pp. 122–127.
29. Klug, H.P. and Alexander, L.E., *X-Ray Diffraction Procedures for Polycrystalline and Amorphous Materials*, New York: Wiley, 1974.